Hydrogen assisted rolling contact fatigue due to lubricant degradation and formation of white etching areas

Dominik Kürten[1], Iyas Khader[2,1], Rahul Raga[1], Paula Casajús[1], Nicholas Winzer[1], Andreas Kailer[1], Reiner Spallek[3], Matthias Scherge[1]

[1] Fraunhofer Institute for Mechanics of Materials IWM, Fraunhofer-KIT MicroTribology Center µTC, Wöhlerstr. 11, 79108 Freiburg, Germany

[2] Department of Industrial Engineering, German-Jordanian University, P.O. Box 35247, 11180 Amman, Jordan

[3] Klüber Lubrication München SE & Co. KG, Geisenhausener Strasse 7, 81379 München, Germany

Abstract

RCF tests were conducted on bearings lubricated with three different lubricants: a gearbox oil, a MAC fluid and PFPE oil. The decomposition of the MAC fluid and PFPE was investigated by FTIR and NMR. Gearbox oil tests showed flaking and networks of subsurface cracks with partial intercrystalline crack growth. Cross-sectional analysis revealed the formation of WEAs. FEM correlated the damage with stress fields. The results of the MAC lubricated tests showed surface flaking and intercrystalline crack growth in the subsurface. The PFPE lubricated bearings showed no signs of hydrogen induced damage.

Post-experimental hydrogen analysis of the bearings indicated an increased hydrogen concentration in the samples lubricated with the gearbox oil and MAC compared to those lubricated with PFPE.

Keywords: Hydrogen embrittlement, RCF, lubricant degradation, WEA/WEC, CRTB

1 Introduction

Rolling contact fatigue (RCF) of bearings is often manifested by subsurface cracking and eventual spalling [1]. RCF in martensitic steel is often associated with a transformation of retained austenitic to martensitic phase [2]. This transformation has been shown to reach its peak in the region of maximum shear stresses below the surface [3], where micro plastic deformation accumulates. Voskamp and Mittemeijer [4] and Swahn et al. [5] observed the development of a dark etching region (DER) in the zone of the highest shear stresses under rolling contact [6]. These structural changes were reported to form globular and elongated grains [7]. During the formation of the DER, a heavily deformed ferrite phase [5] was observed in the martensitic matrix in the form of white bands as low angle bands (LABs) and high angle bands (HABs). The formation of these white bands is often observed along with the development of residual stresses, decrease in hardness [8], and spalling on the rolling surface.

The presence of hydrogen in steel undergoing rolling contact may lead to early fatigue failure [9, 10]. The role played by atomic hydrogen in promoting a self-diffusion processes in iron that accelerates fatigue damage [9] was proposed as one possible explanation. Hydrogen induced damage is often associated with the formation of white etching areas (WEAs), which are correlated to brittle flaking [10]. Evidence has shown that white etching areas (WEA) and white etching cracks (WEC) are initiated at voids or inclusions by linking butterflies or small WECs into networks of WECs [11]. These can eventually propagate to the surface and cause white structure flaking (WSF). FIB 3D-tomography of WEAs indicated a BCC nanocrystalline ferrite structure, which contains different phases like inclusions and spherical iron chromium carbides [11]. It was argued that such nanocrystalline ferrite grains are produced in a low temperature recrystallization process [12, 13]. It was shown that shear induced local plastic

deformation occurs during the formation of WEAs [14].

Tamada and Tanaka [10] proposed that brittle flaking was formed due to hydrogen release by lubricant degradation. Lubricant degradation and hydrogen evolution are greatly enhanced due to high slip and boundary lubrication [15], which result in chemical aging of the lubricant and the formation of an acidic fluid, which in turn attacks the steel surface [16]. It was demonstrated through oxidation tests that hydrogen is produced in an oxidation reaction of the lubricant with the steel surface [17]. On the other hand, wear induced nascent surfaces and tribofilms create ideal sites for hydrogen adsorption [18, 19]. The mechanisms for hydrogen generation in multiply-alkylated cyclopentanes (MAC) lubricated ball-on-plate vacuum tribometer tests were evaluated by in-situ analysis of gaseous reaction products with a mass spectrometer [20, 21, 22, 23, 24, 25]. Lubricant degradation is caused by a tribochmical reaction of the lubricant with nascent metal surface. As a product of the degradation reaction lubricant fragments like H_2^+, CH_3^+, $C_2H_3^+$, $C_2H_4^+$, and $C_3H_7^+$ were formed [20, 21, 22, 23, 24, 25, 26]. Additional oxidation reaction products of the lubricant and the metal oxide layer like esters, ethers, and carboxylic acids were detected [24, 27, 28, 29, 30].

The aim of the present study is to investigate rolling contact fatigue, hydrogen embrittlement and lubricant degradation in a cylindrical roller thrust bearing (CRTB) lubricated with a commercial gearbox oil, MAC fluid, and PFPE oil. The uniqueness of this work lies in correlating the degradation of various lubricants with the hydrogen content of the bearings tested in full scale endurance tests and to explain the damage by relying on numerical simulations.

2 Experiments and analytic methods

Two CRTB types: 81212-TV and 81112-TV made of 100Cr6 steel (AISI 52100) from Schaeffler Technologies AG & Co. KG were used to run rolling-contact fatigue tests. The elemental composition of the bearing steel was analyzed in [25] by glow discharge optical emission spectroscopy (GDOES), Table 1.

Table 1: Elemental composition of bearing steel 100Cr6 **[25]**

Cr	C	Mn	Si	Mo	V	Fe
1.52±0.03	1.08±0.02	0.33±0.02	0.26±0.03	< 0.1	< 0.1	balance

The tests were performed with a normal load of 60 kN (1.4 GPa maximum Hertzian contact stress) at a rotational speed of 750 rpm in the case of the 81212-TV and with a normal load of 50 kN (1.7 GPa maximum Hertzian contact stress) and a rotational speed of 250 rpm in the case of the 81112-TV. The rolling contact fatigue tests were performed using three different lubricants: a commercial gearbox oil (three tests on 81212-TV), a 1,2,4-Tris (2-octyl- 1-dodecyl) cyclopentane (MAC) from Nye Lubrication (two tests on 81112-TV) and a perfluoro-poly-ether (PFPE) from Klüber Lubrication (two tests on 81112-TV). The chemical structure of the MAC fluid and PFPE oil are shown in **Figure 1** and **Figure 2**, respectively.

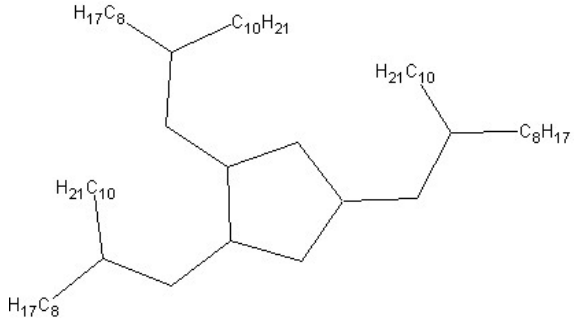

Figure 1: Chemical structure of MAC (multi-alkylated-cyclopentane) [24].

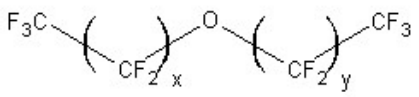

Figure 2: Chemical structure of PFPE (perfluoro-poly-ether) [24].

The viscosities of the lubricants are: Gearbox oil: 64 cSt (40 °C) and 9.5 cSt (100 °C); MAC fluid: 108 cSt (40 °C) and 14.6 cSt (100 °C); and PFPE oil: 100 cSt (40 °C) and 14 cSt (100 °C).

A summary of the experimental parameters are shown in Table 2.

Table 2: Experimental parameters of the RCF tests

Test series no.	**1**	**2**	**3**
Bearing type	81212-TV	81112-TV	81112-TV
Lubricant	Gearbox oil	MAC fluid	PFPE oil
Tested bearings	3	2	2
Running temperature (self-heating)	90 °C	75 °C	120 °C
Load (kN)	60	50	50
Rotational velocity (rpm)	750	250	250
Viscosity ratio	0.57	0.53	0.12
Test duration (h)	50*	115**, 460***	230**, 1170**
No. of load cycles on each roller (10^6)	15.9	16.7, 66.6	33.3, 169.4
No. of load cycles on each race (10^6)	21.38	93.15	236.93

* Fixed test duration

** Test stopped manually for inspection

*** Test stopped automatically due to bearing failure

Scanning electron microscopy (SEM) and electron backscatter diffraction (EBSD) were carried out on a Zeiss Supra 40VP scanning electron microscope. Samples for optical microscopy, SEM and EBSD were prepared by grinding with up to 1200-grade emery paper and polishing with 0.25 µm diamond paste. The samples were then etched with acetic picral reagent (to reveal grain boundaries) or nital (to reveal WEA structures). To reach a deformation free surface for the EBSD analysis the samples were finally polished with colloidal silica (OPS) with 0.04 µm for 12 min. The hydrogen concentration of the cylindrical rolling elements was analyzed with carrier hot gas extraction. The hydrogen

content of the rolling elements was measured normalized by their weight. The analyzer was calibrated with at least 15 calibration samples with a predefined hydrogen concentration of 1.9 ppm. Three cubes in dimensions of 5×5×5 [mm] were cut from the surface-near material of the rollers and races by electric discharge machining from each tested bearing directly after finishing the test. The samples were degreased with acetone and n-hexane and any oxide/recast layer was removed by slightly grinding off the surface with emery paper. The analysis was carried out by completely melting the samples in the analyzer. The samples for the X-ray photoelectron spectroscopy (XPS) were washed either with n-hexane (for MAC fluid) or tetradecafluorohexane (for PFPE oil) in order to selectively remove the oil layer from the surface without removing reaction products. For the XPS analysis a Phi 5000 VersaProbe from Physical Electronics with a 15 keV Al K-alpha X-ray source was used. The depth profile was sputtered with argon ions accelerated with an energy of 1 eV – 3 eV. The sputter rate was calibrated on a silicon oxide calibration sample with a thickness of 100 nm. Nuclear magnetic resonance spectroscopy (H-NMR) (300 MHz, 128 scans, samples solved in $CDCl_3$) and Fourier-transform infrared spectroscopy (FTIR) analyses of lubricants were carried out. A tetramethylsilane internal standard was used for spectral calibration for NMR.

3 Finite element analysis

Finite element (FE) simulations of the contact in the CRTB 81212-TV were performed through a quasi-static analysis in Abaqus/standard. The geometry of the model was simplified to consist of four rolling elements separated by a polyamide (PA-66) cage. The upper race was rotated while fixing the lower race. A Coulomb friction model with a constant coefficient of friction of μ=0.15 was adopted to model friction. Eight-node first-order hexahedral elements with displacement degrees of freedom were used to

discretize the geometry. A fine mesh was used to discretize the contact zones with an average element size of 250×85×85 [µm], Figure 3.

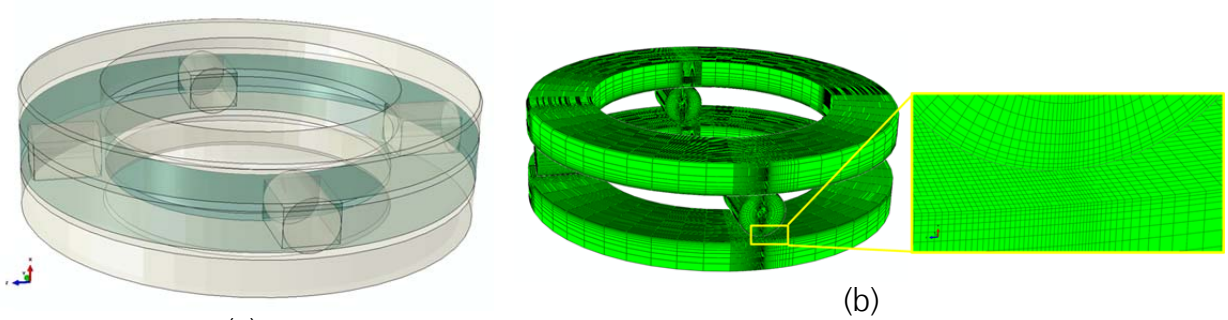

(a) (b)

Figure 3: Finite element model of the CRTB.

The profile geometry of the rollers was assumed to be flat. The elastic modulus and Poisson's ratio for 100Cr6 were assumed to be 212.0 GPa and 0.29, respectively. Polyamide (PA 66) was modeled with an elastic modulus and Poisson's ratio of 3.95 GPa and 0.39, respectively.

4 Results

4.1 Rolling contact fatigue tests with a commercial gearbox lubricant

After completion of the RCF tests with the 81212-TV CRTBs lubricated with gearbox oil, damage analysis of the rollers was performed to characterize the extent of damage. All tested bearings showed damage signs after the 50 h test duration. In **Figure 4a**, surface flaking on the rolling elements was observed. **Figure 4b** shows an SEM micrograph of the damage on the bearing raceway.

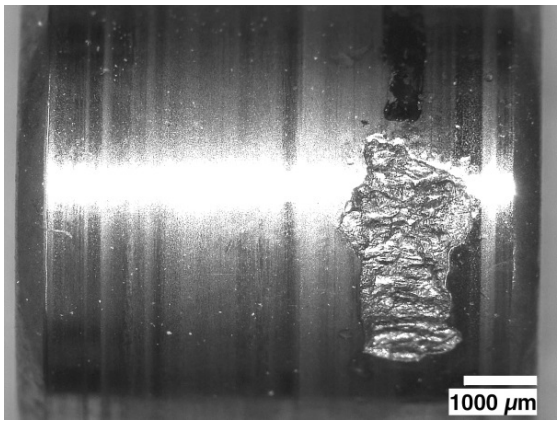

(a)

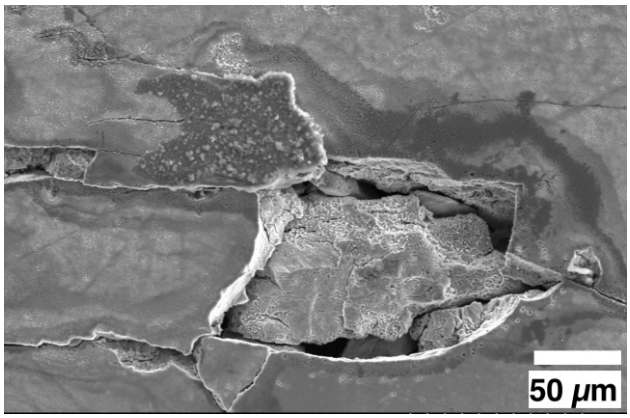

(b)

Figure 4: Damage on a 81212-TV bearing after conducting the RCF test. a) Flaking damage on the rolling element, b) SEM micrograph of surface damage on the raceway. Lubricant: gearbox oil.

Figure 5a shows a cross section prepared across a flaking site in a rolling element (similar to **Figure 4a**). Subsurface circumferential crack growth is observed on the left side of the image. In this region, the rolling surface is still visible and surface and subsurface cracks coalesce. Flaking damage in the middle and right side of the image are also visible, wherein cracks develop and grow into the depth. Radial cracks undergo transcrystalline growth near the surface, which gradually becomes predominantly intercrystalline along retained austenitic grains (cf. Šmeļova et al. [31]) especially at the crack tip, as detailed in **Figure 5b**.

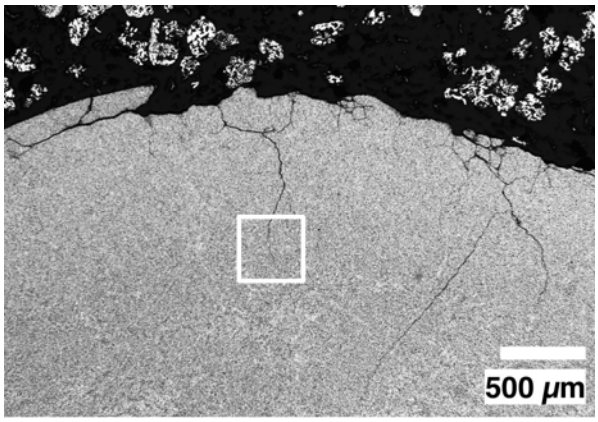

(a)

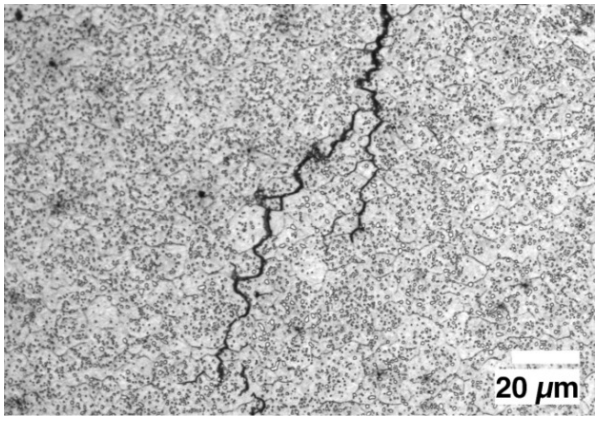

(b)

Figure 5: Optical micrographs of the cross section of a rolling element etched with picric acid. a) Overview of flaking damage site showing surface and subsurface crack growth, b) detailed view of the crack tip. Lubricant: gearbox oil.

Cross sections at seemingly intact surface regions were prepared, **Figure 6a**. A network of subsurface WECs was observed. On several occasions, WEAs appear adjacent to the cracks along with what appears to be deformation zones (region 2 in **Figure 6b**). Crack growth appears to be mostly transcrystalline with intercrystalline growth in some regions (e.g., regions 3 in **Figure 6b**). WEAs were mostly observed on one side of the cracks in the transcrystalline crack growth regions (region 1 in **Figure 6b**). The formation of DER under the rolling surface was not observed.

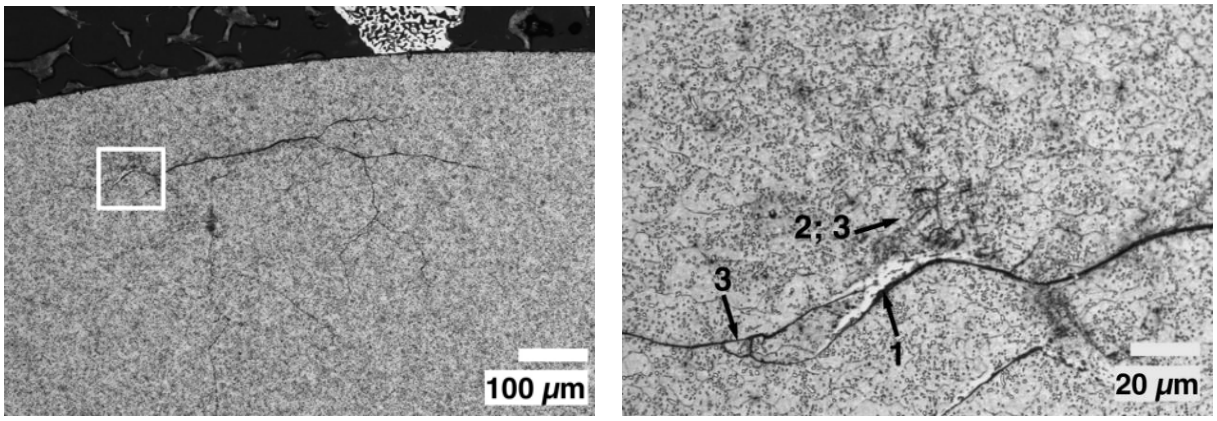

(a) (b)

Figure 6: Optical micrographs of the cross section of a cylinder rolling element etched with picric acid. 1) Overview of WEA, 2) deformation zone, 3) intercrystalline crack growth. Lubricant: gearbox oil.

SEM cross-sectional analysis in backscatter mode of a rolling element is shown in **Figure 7**. The formation of WEA and subsurface cracks in depths ranging between 90 µm and 130 µm was observed, **Figure 7a**. Radial surface initiated cracks were observed in some cases as indicated by the arrows in **Figure 7a**. Numerous microcracks can be also be observed within the WEA (**Figure 7b**).

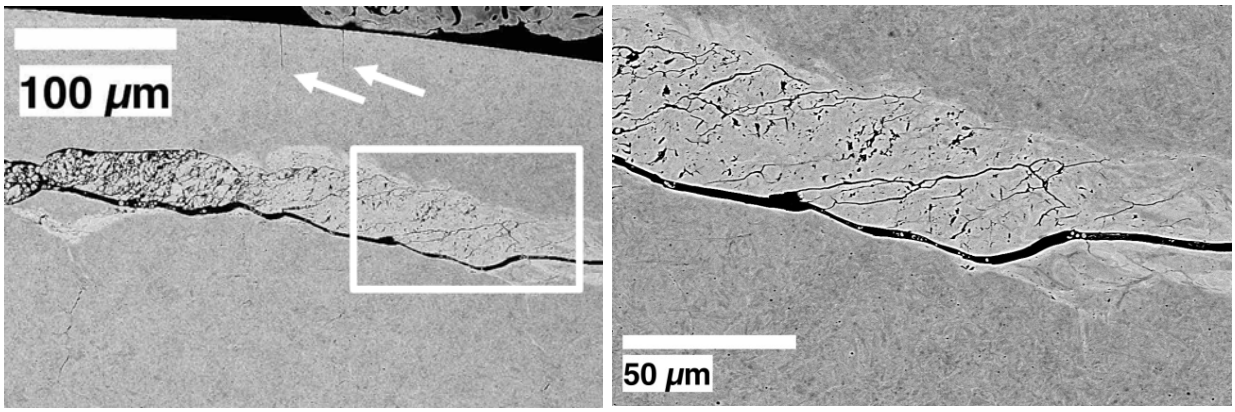

(a) (b)

Figure 7: Backscatter SEM micrographs of a cross section of a rolling element. a) Subsurface cracks and WEA formation; arrows point to surface initiated cracks. b) Detailed view of the WEA showing microcracks. Lubricant: gearbox oil.

The FE calculated stress fields showed maximum contact pressure of approximately 1.4 GPa of this particular case. Asymmetric tensile stress distribution emerges during rolling contact with a peak value of ca. 150 MPa appearing on the surface, 500 – 750 µm away from the edge of the roller; a filleted or chamfered edge (not considered here) would most probably shift the location of the peak tensile stress further away from the edges towards the center of the roller. Subsurface tensile stresses are in the range of 50 to 60 MPa, **Figure 8**. Due to relative peripheral velocities between the roller and raceway, slip occurs during operation.

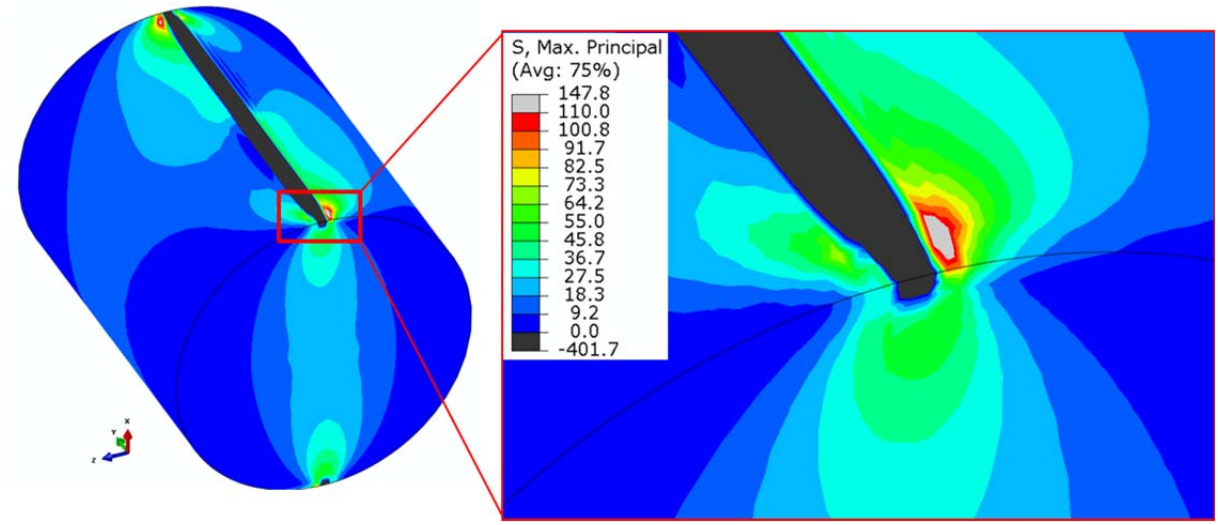

Figure 8: Maximum principal stress (tensile) on the surface of the rolling element.

The von Mises stresses, Figure 9, showed a peak value at the roller surface edges of ca. 940 MPa. A stress gradient appears in the subsurface as well. A maximum subsurface shear stress of 450 MPa appeared ca. 50 µm below the surface.

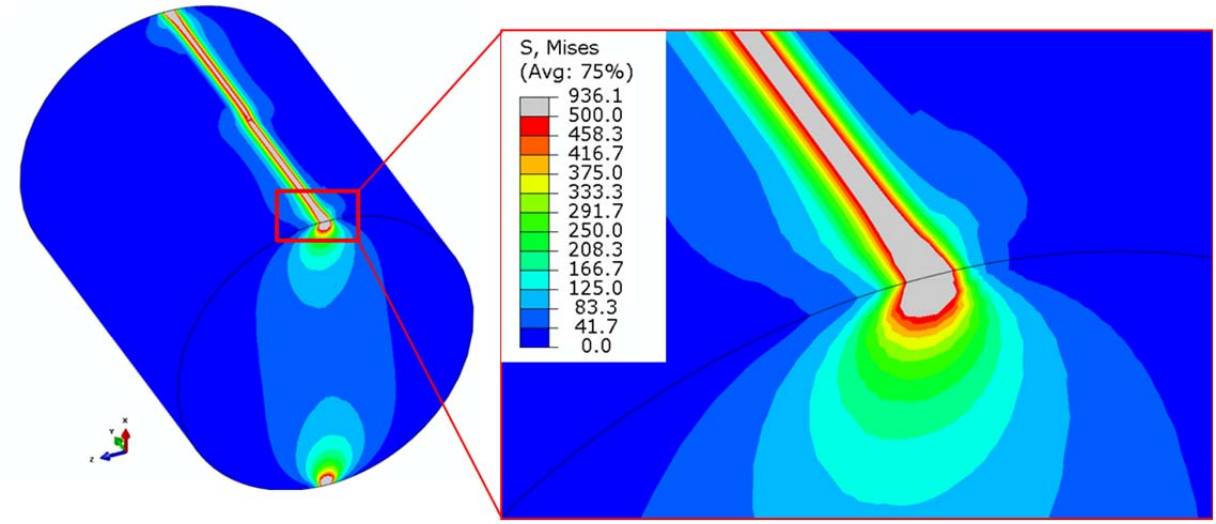

Figure 9: von Mises stress distribution on the rolling element.

Figure 10a shows a zone of WEA in a cross section of a specimen after etching with nital. The transitional region between the WEA and the martensitic phase indicates grain refinement (will be further investigated by EBSD) and dissolving equiaxed carbides (**Figure 10b**).

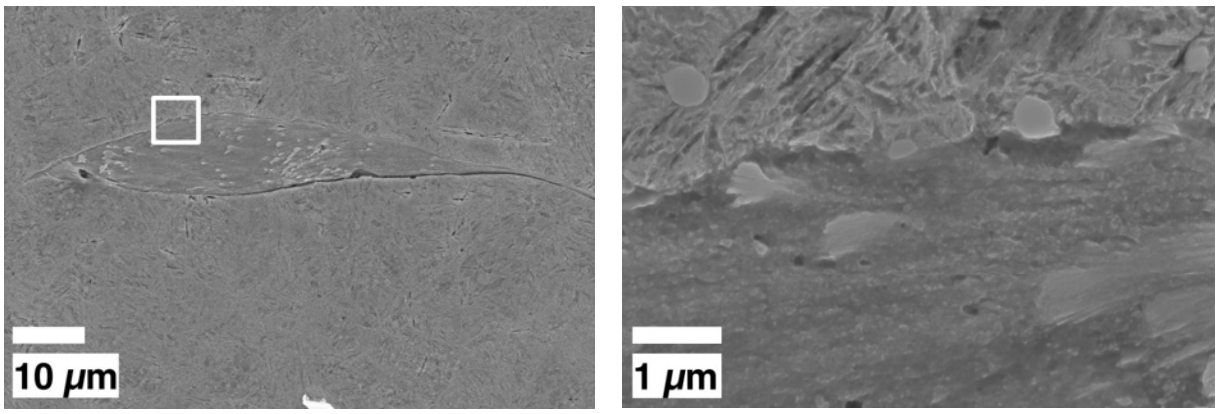

(a) (b)

Figure 10: SEM micrographs of a cross section in a rolling element. a) WEA formation in the subsurface region, b) detailed view of the transitional region between the WEA and bulk material. Lubricant: gearbox oil.

The EBSD map of a WEA on a subsurface crack is shown in **Figure 11**. The scanned area for the EBSD analysis is presented in **Figure 11a**. The grain structure and grain orientation are illustrated in **Figure 11b**. Non-indexed points were observed in the area

of the sample that corresponds to the WEA indicating ultra-fine grain structure. The indexed points in the WEA may correspond to the equiaxed carbides observe in the cross sectional analysis. Grain refinement in the areas close to the WEA may also be observed.

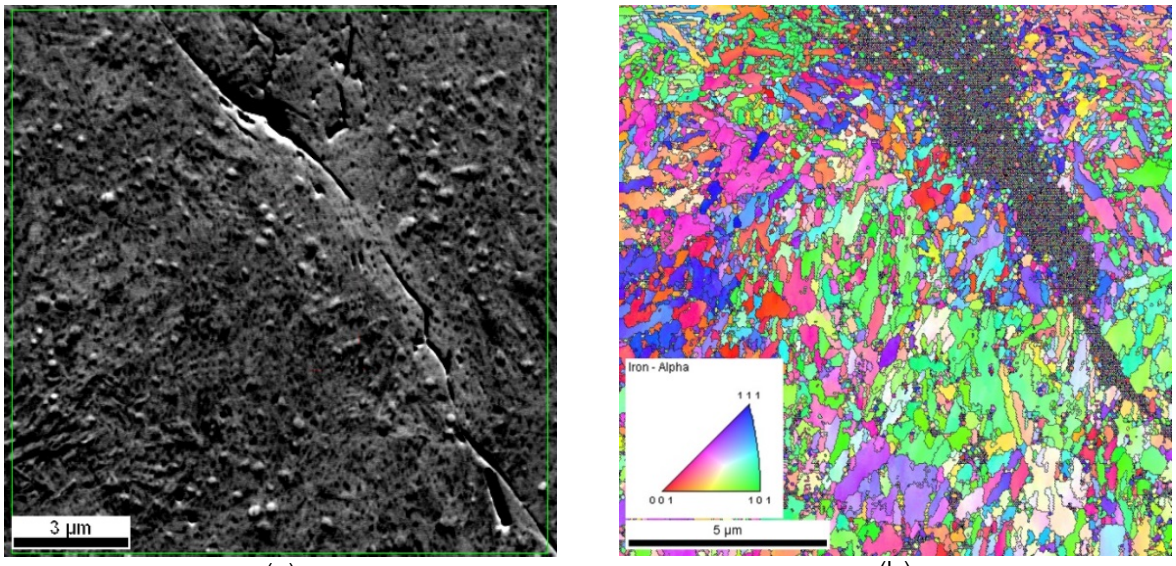

(a) (b)

Figure 11: EBSD analysis of a WEA. a) Scanned region, b) EBSD map. Lubricant: gearbox oil.

Additional EDX analyses showed no significant differences between the WEA and the surrounding matrix material regarding the concentration of the alloy elements (Fe, Cr and Mn).

4.2 Rolling contact fatigue test with MAC fluid

The 115 h RCF test did not indicate any signs of damage; whereas, the 460 h test automatically stopped due to vibrations caused by bearing failure. Further analysis was only conducted on the bearing tested for 460 h. **Figure 12** shows the damage resulting on the 81112-TV bearing. The bearing rollers and races showed flaking damage on the surface.

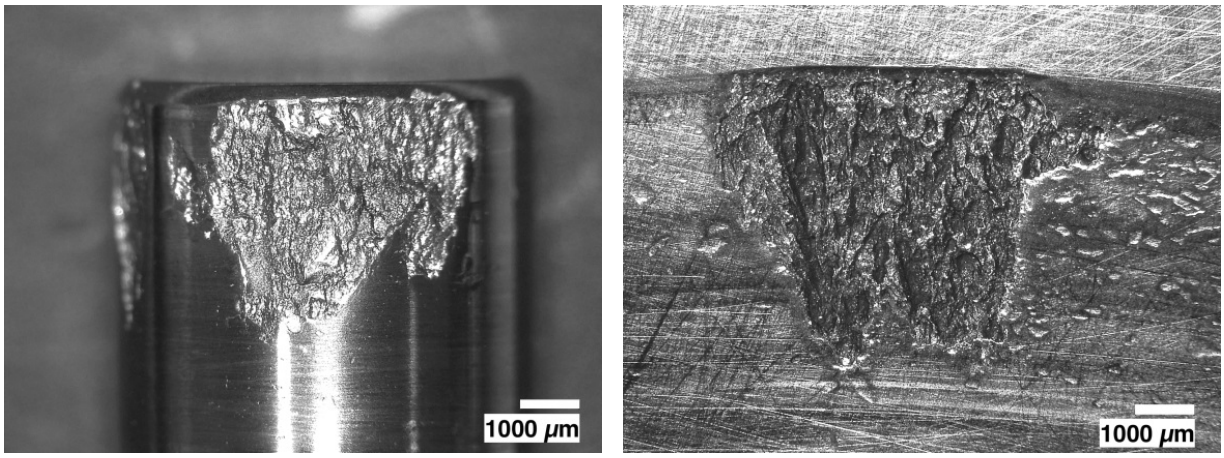

(a) (b)

Figure 12: a) Flaking damage on a cylinder roller and b) on the bearing race of a CRTB after a rolling contact fatigue test with MAC fluid.

Optical microscopy of an etched cross section with acetic picral reagent of a roller is shown in **Figure 13**. An overview of the subsurface crack growth is shown in **Figure 13a**. A circumferential subsurface crack was formed 100 µm under the rolling surface in an area were a deformation layer (DER in **Figure 13a**) was observed. Close to the main circumferential crack, smaller cracks appeared. Transcrystalline crack growth appeared to be dominant with intercrystalline crack growth appearing in some regions especially at crack tips, **Figure 13b.**

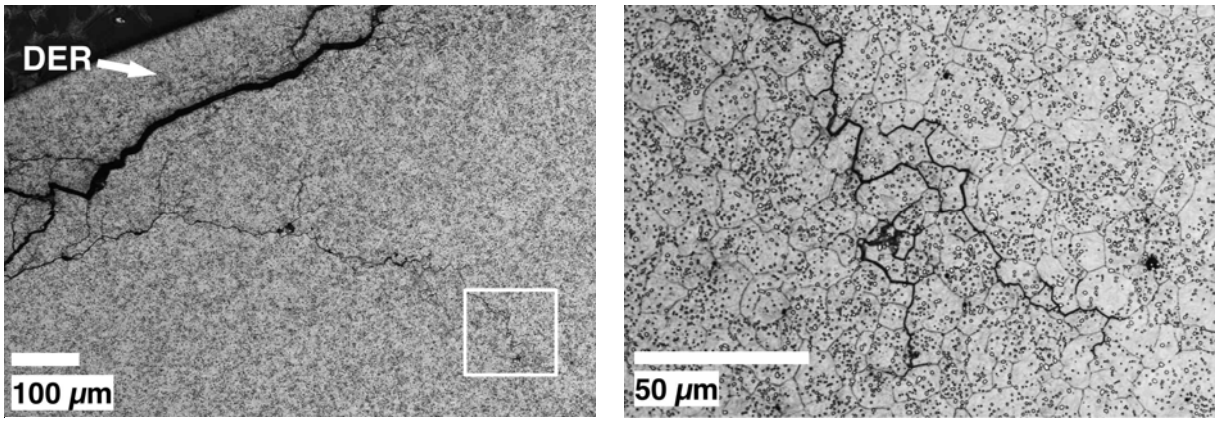

(a) (b)

Figure 13: Cross-sectional analysis of a rolling element etched with picric acid. a) Formation of DER and circumferential subsurface crack growth. b) Dominant intercrystalline crack growth observed at crack tips. Lubricant: MAC fluid.

Figure 14 shows a picral etched cross section of a rolling element. DER formation was observed 50 µm to 400 µm below the surface, **Figure 14a**, with highest intensity

appearing between 70 µm and 250 µm. The deformation occurred mostly within austenite grains, **Figure 14b**.

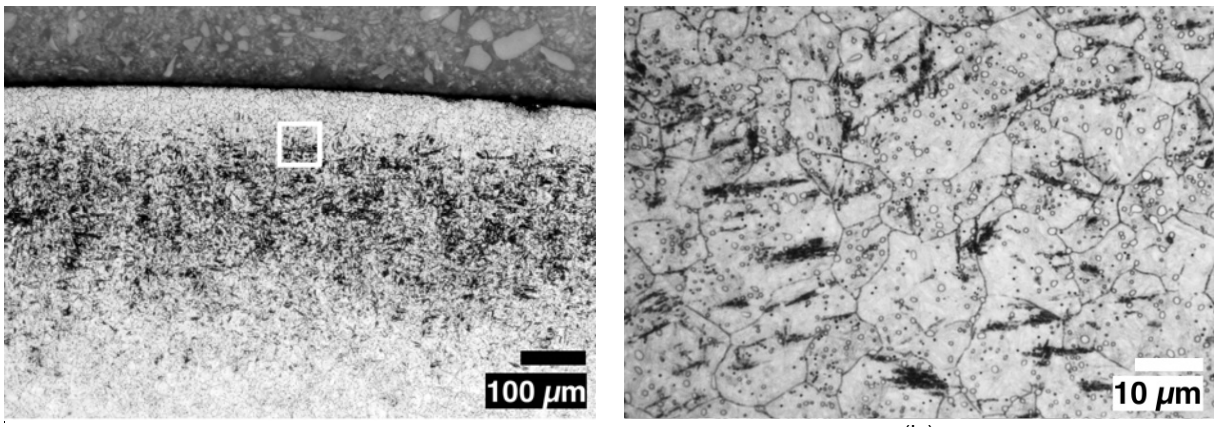

(a) (b)

Figure 14: Picral etched cross section of a roller. a) Formation of DER in the subsurface. b) Deformations within austenite grains; spherical carbides appear as circular features throughout the microstructure. Lubricant: MAC fluid.

XPS analysis was conducted inside the raceway and on the unloaded surface (**Figure 15**) of a bearing race after running the MAC lubricated RCF tests. Degradation reaction products of the lubricant like carboxylic acids (O=C), esters (O=C-O) and ethers (C-O-C) in addition to traces of the lubricant (C-C) appeared on the raceway, **Figure 15**. Similar results were obtained just outside the raceway (unloaded region).

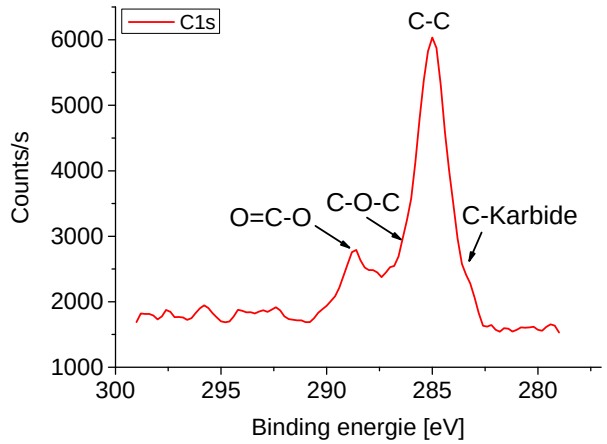

Figure 15 XPS analysis of a bearing surface after the RCF tests with MAC fluid - Inside the raceway.

In a further XPS analysis of the bearing, a depth profile inside (**Figure 16a**) and outside (**Figure 16b**) the raceways were acquired. Higher oxygen and iron oxide concentrations were observed inside the raceway. In both depth profiles, traces of the lubricant were found on the surface. The concentrations of alloying materials like carbon (5 at.%) and chrome (1.5 at.%) are comparable to their standard concentrations in the same type of steel.

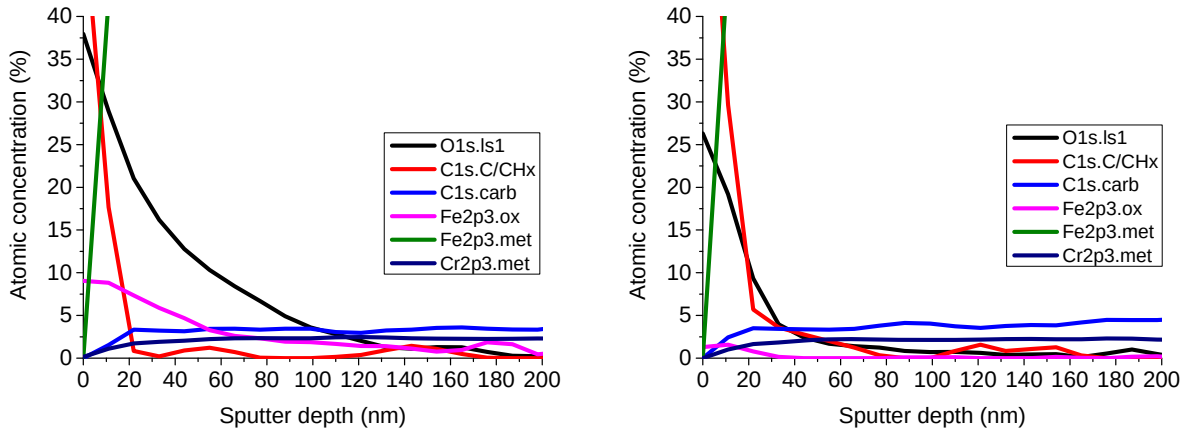

Figure 16: XPS depth profile of a bearing surface after the RCF tests with MAC fluid. (a) Inside and (b) outside the raceway.

A sample of the used lubricant was analyzed with FTIR and NMR after conducting the RCF test. The FTIR analysis indicated reaction products of an oxidation reaction due to the formation of ethers (1300 cm^{-1} – 1000 cm^{-1}), esters (1750 cm^{-1} - 1735 cm^{-1}) and carboxylic acids (1730 cm^{-1} – 1700 cm^{-1}).

The NMR analysis indicated an oxidation reaction to have occurred during the RCF test; esters (2 ppm – 2.2 ppm) and carboxylic acids (2 ppm – 2.7 ppm) were detected. The lubricant in the virgin state was also analyzed and only methyl, methylene and methin protons, in addition to unfunctionalized and saturated hydrocarbons were detected (0.5 ppm – 2.5 ppm).

4.3 Rolling contact fatigue test with PFPE oil

RCF tests on a 81112-TV bearing with PFPE oil were carried out for 230 h and 1170 h, after which they were stopped to analyze the damage on the bearing. The surface analysis, **Figure 17a** and **b** indicated no sign of damage on either the rolling elements or the races. Further analysis was only conducted on the bearing tested for 1170 h.

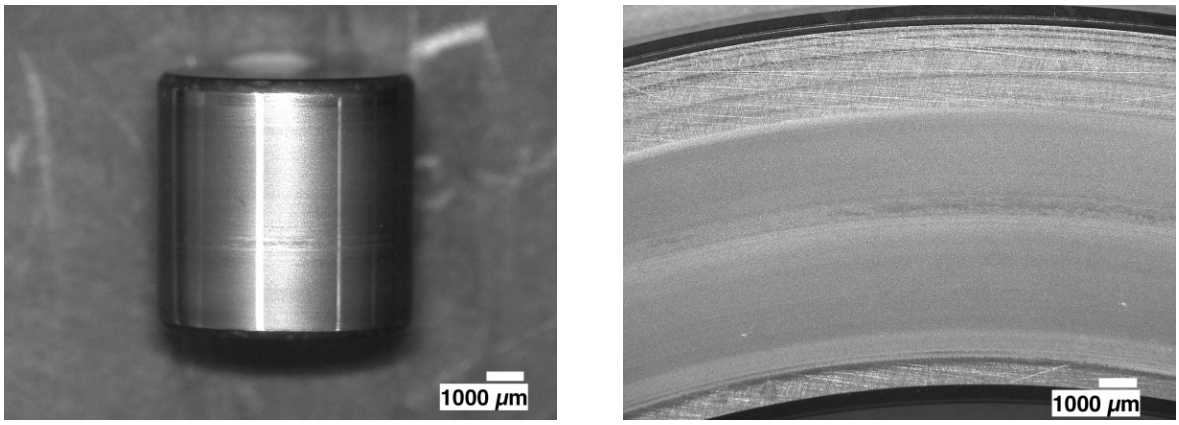

(a) (b)

Figure 17 Optical microscopy of a 81112-TV CRTB after an RCF test with PFPE oil. (a) Rolling element, (b) raceway.

Figure 18 shows an SEM image of the bearing race. The transitional region between the raceway and the unloaded surface appears in the image. Polishing grooves are still visible on the unloaded surface region of the race. A detailed view shows what appear to be corrosion products on the raceway.

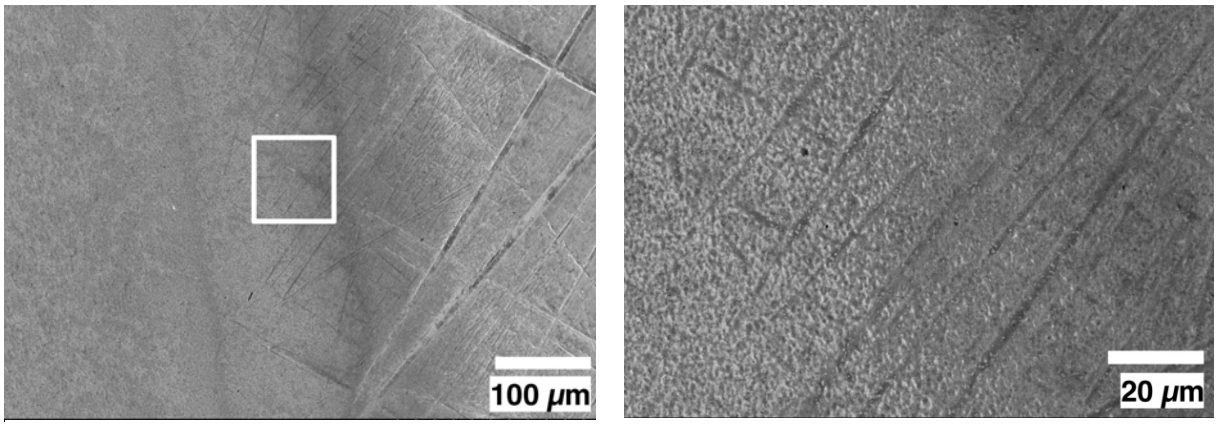

(a) (b)

Figure 18 SEM analysis of the bearing race. (a) Transitional region between the raceway and the unload surface, and (b) detailed view of the surface. Lubricant: PFPE oil.

The picral etched cross-sectional analysis of tested rolling elements, **Figure 19**, indicated the formation of DER in the subsurface. The DER appears 50 µm – 200 µm below the surface and mostly within retained austenite grains.

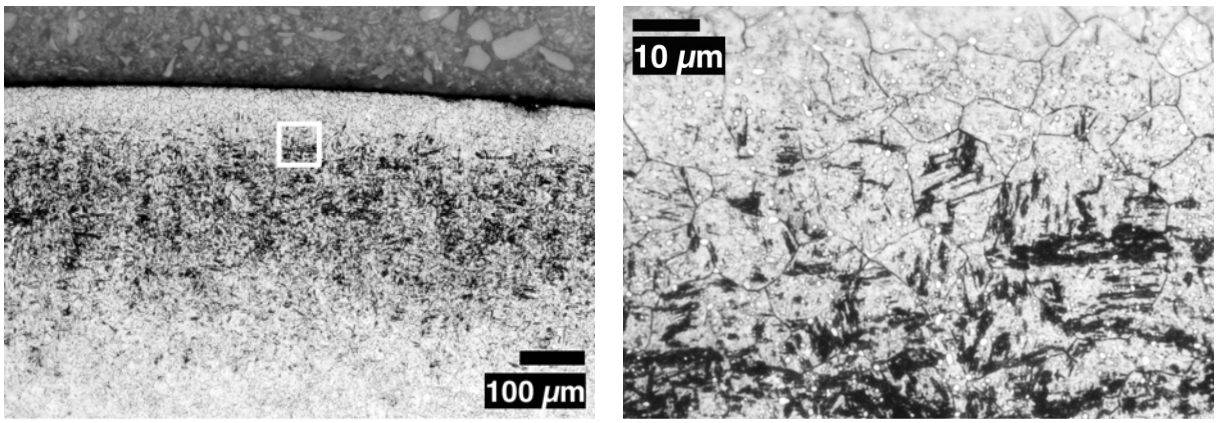

(a) (b)

Figure 19 Picral etched cross section of a cylinder roller. Formation of a DER under the race. a) Formation of a DER under race. Section without subsurface crack growth. b) Development of deformations in the austenite grains. Lubricant: PFPE oil, test duration: 1170 h.

Post experimental XPS surface analysis was carried out; both surfaces, inside the raceway (**Figure 20a**) and in the unloaded region of the race (**Figure 20b**) were analyzed. The XPS analysis indicated fluorocarbons (traces of the PFPE oil) in both regions.

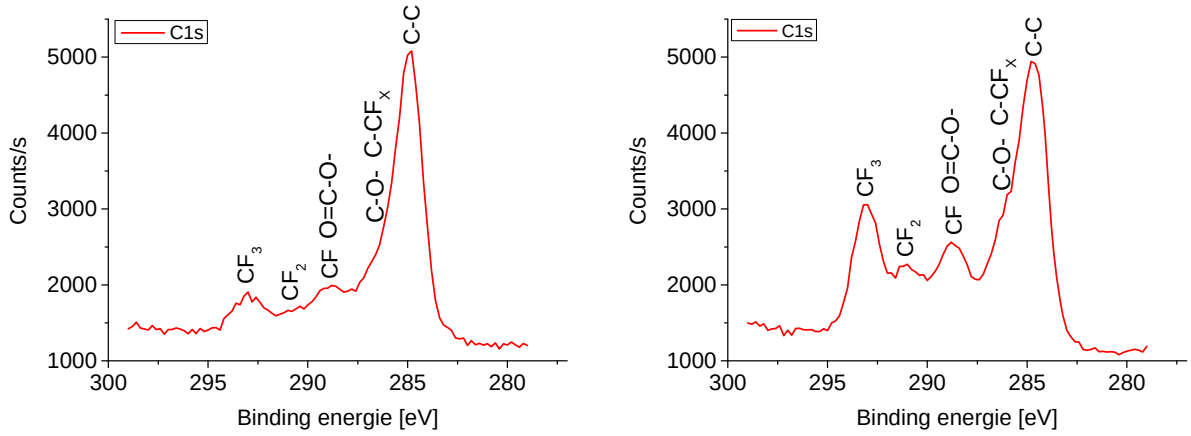

Figure 20 XPS analysis of the bearing surface after the RCF tests with PFPE oil. (a) Inside the raceway and (b) in the unloaded surface of the race.

A depth profile analysis of the race showed iron fluoride complex (F1s.FeF_x), **Figure 21**. This occurs through a corrosion reaction of the lubricant with the iron surface of the bearing.

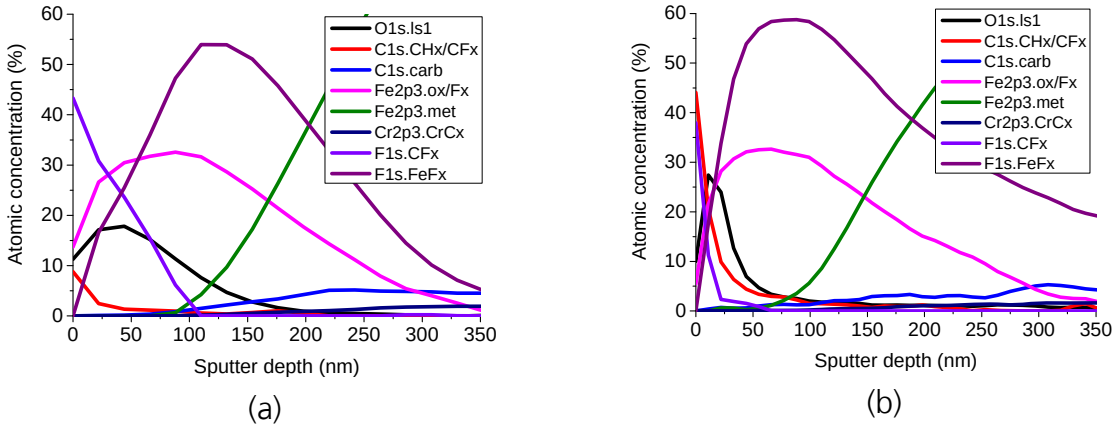

Figure 21 XPS depth profile of the bearing surface after the RCF tests with PFPE oil. (a) Inside and (b) outside the raceway.

4.4 Analysis of hydrogen content

The hydrogen content after conducting the RCF tests was measured as detailed in Section 2 and compared to virgin samples. **Table 3** lists the results of the carrier gas hot extraction measurements on all samples. The hydrogen concentration was normalized by the weight of the samples. All bearings showed increased hydrogen concentration after conducting the RCF tests. The highest concentration was found in samples

lubricated with the gearbox oil followed by those lubricated by the MAC fluid. The samples lubricated with PFPE oil showed hydrogen concentration close to that in virgin samples.

Table 3: Carrier gas hot extraction results

Sample (test duration)	Averaged hydrogen concentration [ppm]	Standard deviation [ppm]
Bearing race (virgin)	0.9	0.1
Gearbox oil (50 h)	2.7	0.1
MAC fluid (460 h)	1.9	0.1
PFPE oil (1170 h)	1.2	0.1

5 Discussion

The bearings tested with commercial gearbox oil showed brittle flaking damage on the surface. The damage was located in regions showing the highest tensile stresses as confirmed by the FE simulations, compare **Figure 4** and **Figure 8**. Tensile stresses in rolling contact are influenced by friction and slip between the rolling element and race, which explains their asymmetric distribution. Subsurface regions undergoing high von Mises stresses (**Figure 9**) coincided with WEAs observed in SEM cross-sectional analysis, **Figure 10**. It was reported by Gould et al. [32] that WECs in wind turbine bearings propagate beneath the raceway in the subsurface region without reaching its surface. This indicates that ingress of lubricant into the crack is not necessary to form WECs. Vegter and Slycke [9], on the other hand, showed in comparison tests between hydrogen charged and uncharged samples that the formation of WECs was only observed in the hydrogen charged bearings, whereas WECs were not formed in their uncharged counterparts. It is hence argued that in this specific case, WEAs and WECs appear to be hydrogen induced forms of damage.

The EBSD analysis of a WEA shows an ultrafine structure, which cannot be detected by EBSD. On the interface between the WEA and martensitic matrix, grain refinement was also observed. Literature findings point out that WEA has an ultrafine, nanocrystalline grain structure, which develops through a recrystallization process at low temperatures [12, 13]. The micrographs obtained by SEM show that the WEA comprises a very fine structure of nanoparticles. This is in agreement with Evans et al. [11], who showed in a 3D FIB analysis of a WEA that it consists of nanocrystalline BCC ferrite containing different phases such as inclusions or spherical carbides. One hypothesis concerning the formation of WEAs is that they form due to crack face fretting under the effect of cyclic load in rolling contact [9]. Another explanation may be given in terms of slip induced shear stresses, which were reported to have a significant influence on the formation of WEAs [14].

In regions of high subsurface von Mises stresses, transcrystalline crack growth predominates over the intercrystalline. WEAs were mostly observed in the vicinity of transcrystalline cracks growth. Radial cracks are thought to propagate in mode I under the effect of high surface-near tensile stresses and undergo transcrystalline crack growth. At higher depths, where stresses are low enough, crack propagation becomes mostly intercrystalline. Such cracks are assumed to be hydrogen influenced and are the main cause for flaking damage; an increased hydrogen concentration by ca. 1.8 ppm after running the RCF tests supports this assumption.

The samples tested with MAC fluid showed comparable results to what was observed in the tests conducted using the commercial gearbox oil. Intercrystalline crack growth was observed (**Figure 13**), which is an indicator for hydrogen influenced damage, whereby hydrogen promotes crack growth along grain boundaries. The absence of WEA in the

MAC fluid lubricated tests may be attributed to the rather low hydrogen content measured after running the RCF tests (compare values in **Table 3**). The gearbox oil used in this study is a fully-formulated oil in comparison to the non-additivated MAC fluid; the additive content of the gearbox oil may be the reason behind a higher hydrogen evolution from the lubricant, which resulted in the higher hydrogen content in steel and the formation of WEA (cf. [33, 34]).

In this case however, DER formed below the raceways, wherein circumferential subsurface cracks were observed (**Figure 13a**). DER, an indication of fatigue damage, consists mainly of plastically deformed austenitic grains formed during rolling contact (see **Figure 14**). The micrograph in **Figure 14b** shows darks region within the grains, which are most probably microstructural defects that are highly susceptible to chemical etching (similar behavior is obtained when etching grain boundaries); such regions are described in the literature as DER [6]. Both DER and transcrystalline subsurface cracks form in regions of high von Mises stresses. The duration of the MAC fluid lubricated tests was almost an order of magnitude higher than those run with the commercial gearbox oil, and therefore, fatigue effects (e.g., DER) are more likely to occur.

The XPS surface analysis of MAC fluid lubricated samples along with the NMR and FTIR lubricant analysis revealed an oxidational reaction of the lubricant that resulted in forming carboxylic acids, ethers and esters (**Figure 15**). Carboxylic acid chemically reacts with the metal surface and forms iron carboxylate. During the iron carboxylate formation, hydrogen is produced. Bertrand [28] was able to detect iron carboxylate in a sliding test under vacuum with MAC fluid. **Figure 22** shows the proposed reaction mechanism which leads to the formation of brittle flaking and hydrogen embrittlement of bearing lubricated with non-additivated base oil like MAC.

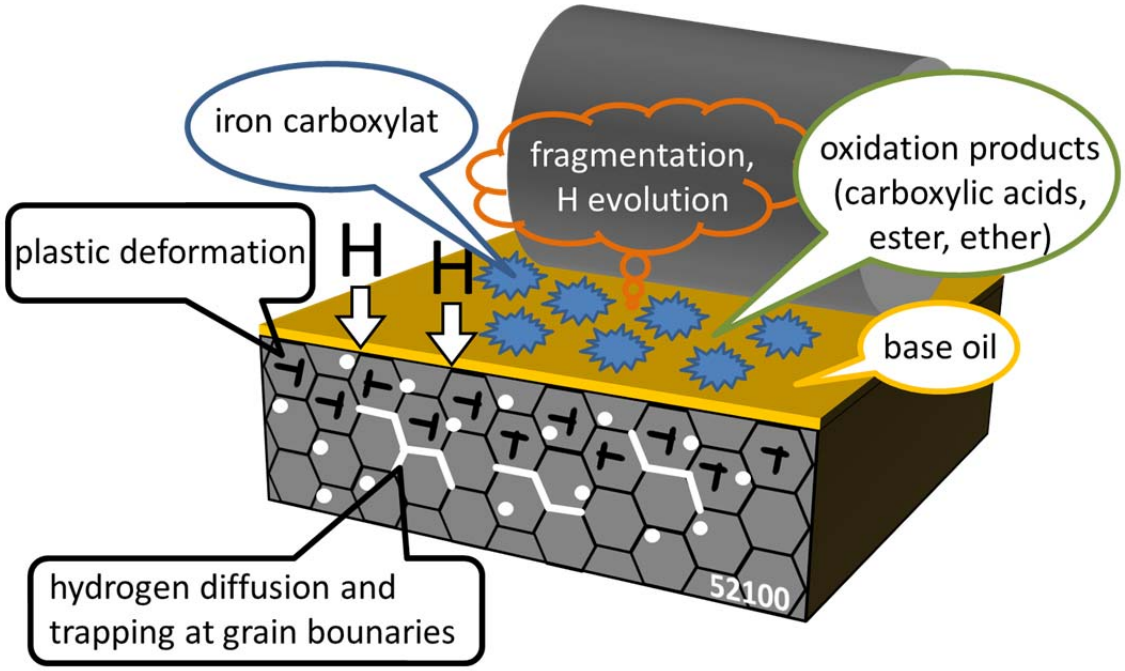

Figure 22: Schematic of the proposed mechanism which leads to hydrogen embrittlement of bearings.

The hydrogen analysis of the bearings after the test with MAC fluid showed an increased hydrogen concentration compared to virgin samples. The XPS analysis (**Figure 15a**) showed the formation of carbidic carbon on the surface. This indicates a fragmentation reaction of the lubricant on the surface during rolling contact, which usually yields low molecular fragments such as alkanes and alkenes in addition to hydrogen (the latter detected under vacuum) [20, 21, 22, 23, 24]. XPS, FTIR and NMR analyses did not confirm the presence of low molecular fragments. It is highly probable that low molecular fragments react with oxygen from the atmosphere to form carboxylic acids, esters and ethers [24, 35, 36]. The XPS depth profile analysis showed an increased concentration of oxygen due to the oxidational reactions of the lubricant with the metal surface and the atmosphere, **Figure 16**.

The bearings lubricated with PFPE oil showed no signs of surface damage. Subsurface cross-sectional analysis revealed the formation of DER in the 1170 h test in regions of high shear stresses (**Figure 19**). DER observed in PFPE oil lubricated samples appeared

wider than those found in MAC fluid lubricated samples, which can be explained in light of the duration of the test. In this case as well, plastic deformation in the DER was mainly formed in the retained austenite grains. The hydrogen concentration found in the bearing tested with PFPE oil may be attributed either to moisture in the lubricant or the atmosphere. It seems that the hydrogen concentration was too low to trigger any damage in the RCF test.

The XPS surface analysis of PFPE lubricated samples showed the formation of oxidational reaction products like carboxylic acid, esters and ethers and/or fragmentation reaction products of the lubricant such as CFx and C-CFx. Both oxidational and fragmentational reaction products overlap in their binding energy (**Figure 20**) and both reaction mechanisms may be attributed to lubricant degradation in a tribological contact. The PFPE lubricant used in the present work is a fully fluorinated lubricant, which lowers the possibility for the formation of a carboxylic acid, ethers and esters due to lubricant degradation. The XPS depth profile analysis of the bearing surface (**Figure 21**) revealed tribochemical reaction products of the metal surface and the lubricant (appears in the SEM image in **Figure 18b**); the corrosion reaction led to the formation of an iron fluoride complex. The results indicated higher concentration of the CFx lubricant fragments (F1s.CFx) than oxygen (O1s) in the first 100 nm. The oxygen concentration inside the raceway appeared to be higher compared to the area outside it. This is probably caused by a lubricant oxidation reaction and the formation of iron oxide within the loaded raceway.

6 Conclusion

Full scale endurance tests were carried out on bearings with three different lubricants: gearbox oil, MAC fluid and PFPE oil. Post-experimental hydrogen analysis of the bearings

indicated highest concentration in the gearbox oil lubricated bearings, following by the MAC fluid lubricated bearings. The PFPE oil lubricated samples showed hydrogen concentrations close to those found in virgin samples. The following was concluded from the tests:

Gearbox oil lubrication: resulted in flaking on the surface and formation of subsurface WEAs. Surface initiated radial cracks were observed in zones of highest tensile stress. In subsurface regions of low von Mises stresses, intercrystalline crack growth was dominant, which is interpreted as hydrogen influenced damage. In contrast, in regions of higher von Mises stresses, transcrystalline crack growth appeared to dominate. The formation of WEAs was only observed in these regions. No sign of fatigue damage was observed.

MAC fluid lubrication: the bearing underwent surface flaking and showed networks of subsurface cracks. Despite showing increased hydrogen content, WEAs were not detected but rather sings of hydrogen induced damage. The high number of load cycles in the RCF tests resulted in fatigue damage in form of DER. The degradation of the MAC fluid led to the formation of carboxylic acids, ethers and esters. A mechanism that leads to hydrogen embrittlement in MAC fluid lubricated bearings was proposed.

PFPE lubrication: did not result in any form of hydrogen induced damage but rather subsurface fatigue damage. This was a result of the high number of the undergone stress cycles. Post-experimental hydrogen analysis showed a concentration almost similar to that measured in virgin samples. Chemical analysis of PFPE oil only indicated the formation of an iron fluoride complex during the RCF test.

Acknowledgements

The authors acknowledge the financial support provided by Daimler AG, Klüber Lubrication München SE & Co. KG and Robert Bosch GmbH.

7 References

[1] F. Sadeghi, B. Jalalahmadi, T. Slack, N. Raje and N. Arakere, "A Review of Rolling Contact Fatigue," *Journal of Tribology,* no. 131, 2009.

[2] H. Schlicht, "Waelzermuedung, Teil 3: Werkstoffverhalten bei Hertz'scher Beanspruchung," *HTM Haertereitechnische Mitteilungen,* vol. 59, pp. 363-373, 2004.

[3] R. Dommarco, K. Kozaczek, P. Bastias, G. Hahn and C. Rubin, "Residual stresses and retained austenite evolution in SAE 52100 steel under non-ideal rolling contact loading," *Wear,* vol. 257, pp. 1081-1088, 2004.

[4] A. Voskampk and E. Mittemeijer, "Crystallographic preferred orientation induced by cyclic rolling contact loading," *Metallurgical and Materials Transactions A,* vol. 27, pp. 3445-3465, 1996.

[5] H. Swahn, P. Becker and O. Vingsbo, "Martensite decay during rolling contact fatigue in ball bearings," *Metallurgical Transactions A,* vol. 7, pp. 1099-1110, 1976.

[6] A. Voskamp, R. Österlund, P. Becker and O. Vingsbo, "Gradual changes in residual stress and microstructure during contact fatigue in ball bearings," *Metals Technology,* vol. 1, no. 7, 1980.

[7] V. Smelova, A. Schwendt, L. Wang, W. Holweger and J. Mayer, "Electron microscopy investigation of microstructural alternations due to classical Rolling Contact Fatigue (RCF) in martensitic AISI 52100 bearing steel," *International Journal of Fatigue,* no. 98, pp. 142-154, 2017.

[8] H. Muro and N. Tsushima, "Microstructural, microhardness and residual stress changes due to rolling contact," *Wear,* vol. 5, no. 15, pp. 309-330, 1970.

[9] R. Vegter and J. Slycke, "The Role of Hydrogen on Rolling Contact Fatigue Response of Rolling Element Bearings," *ASTM International,* vol. 7, p. 12, 2010.

[10] K. Tamada and H. Tanaka, "Occurrence of brittle flaking on bearings used for automotive electrical instruments and auxiliary devices," *Wear,* vol. 199, pp. 245-252, 1996.

[11] M.-H. Evans, J. Walker, C. Ma, L. Wang and R. Wood, "A FIB/TEM study of butterfly crack formation and white etching area (WEA) microstructural changes under rolling contact fatigue in 100Cr6 bearing steel," *Materials Science and Engineering: A,* vol. 570, pp. 127-134, 2013.

[12] A. Grabulov, R. Petrov and H. Zandbergen, "EBSD investigation of the crack initiation and TEM/FIB analyses of the microstructural changes around the cracks formed under Rolling Contact Fatigue (RCF)," *International Journal of Fatigue,* vol. 32, pp. 576-583, 2010.

[13] A. Grabulov, U. Ziese and H. Zandbergen, "TEM/SEM investigation of microstructural changes within the white etching area under rolling contact fatigue and 3-D crack reconstruction by focused ion beam," *Scripta Materialia,* vol. 57, pp. 635-638, 2007.

[14] H. Harada, T. Mikami, M. Shibata, D. Sokai, A. Yamamoto and H. Tsubakino, "Microstructural changes and crack initiation with white etching area formation under rolling/sliding contact in bearing steel," *ISIJ International,* vol. 45, pp. 1897-1902, 2005.

[15] B. Han, J. Binns and I. Nedelcu, "In Situ Detection of Hydrogen Uptake from Lubricated Rubbing Contacts," *Tribology Online,* pp. 450-454, 2016.

[16] J. Gegner and W. Nierlich, "Mechanical and tribochemical mechanisms of mixed friction induced surface failures of rolling bearings and modeling of competing shear and tensile stress controlled damage initiation," *Tribologie und Schmierungstechnik,* vol. 58, pp. 10-21.

[17] J. Ciruna and H. Szieleit, "The effect of hydrogen on the rolling contact fatigue life of AISI 52100 and 440C steel balls," *Wear,* vol. 24, pp. 107-118, 1973.

[18] A. Richardson, M. Evans, L. Wang, R. Wood and M. Ingram, "Thermal Desorption Analysis of Hydrogen in Non-hydrogen-Charged Rolling Contact Fatigue-Tested 100Cr6 Steel," *Tribology Letters,* 2017.

[19] A. Ruellan, F. Ville, X. Kleber, C. Burnet, D. Girodin and J. Cavoret, "Understanding White Etching Cracks in Rolling Element Bearings: Reproduction and Influent Tribochemical Drivers".*STLE 69th. Annual Meeting & Exhibition.*

[20] M. Kohara, T. Kawamura and M. Egami, "{Study on mechanism of hydrogen generation from lubricants}," *{TRIBOLOGY TRANSACTIONS},* vol. 49, pp. 53-60, 2006.

[21] R. Lu, I. Minami, H. Nanao and S. Mori, "Investigation of decomposition of hydrocarbon oil on the nascent surface of steel," *Tribology Letters,* vol. 27, no. 1, pp. 25-30, 2007.

[22] R. Lu, S. Mori, T. Kubo and H. Nanao, "Effect of sulfur-containing additive on the decomposition of multialkylated cyclopentane oil on the nascent steel surface," *Wear,* vol. 267, pp. 1430-1435, 2009.

[23] R. Lu, S. Mori, H. Nanao, K. Kobayashi and I. Minami, "Study on Decomposition of Multialkylated Cyclopentane Oil with Sulfur-Containing Additive on the Nascent Steel Surface," *Tribology Online,* vol. 2, pp. 105-109, 2007.

[24] D. Kuerten, N. Winzer, A. Kailer, W. Pfeifer, R. Spallek and M. Scherge, "In-situ detection of hydrogen evolution in a lubricated sliding pin on disk test under high vacuum," *Tribology International,* pp. 324-331, 2015.

[25] D. Kuerten, "Einfluss der tribochemischen Schmierstoffoxidation auf die wasserstoffinduzierte Wälzkontaktermüdung," vol. PhD Dissertation, Fraunhofer Verlag, 2015.

[26] P. John, J. Cutler and J. Sanders, "Tribological behavior of a multialkylated cyclopentane oil under ultrahigh vacuum conditions," *Tribology Letters,* vol. 9, no. 3-4, pp. 167-173, 2001.

[27] P. A. Bertrand, "Low-Energy-Electron-Stimulated Degradation of a Multiply Alkylated Cyclopentane Oil and Implications for Space Bearings," *Tribology Letters,* 2010.

[28] P. Bertrand, "Chemical Degradation of a Multiply Alkylated Cyclopentane (MAC) Oil During Wear: Implications for Spacecraft Attitude Control System Bearings," *Tribology Letters,* vol. 49, pp. 357-370, 2013.

[29] M. Makowska, C. Kajdas and M. Gradkowski, "Interactions of n-Hexadecane with 52100 Steel Surface Under Friction Conditions," *Tribology Letters,* vol. 13, pp. 65-70, 2002.

[30] C. Kajdas, M. Makowska and M. Gradkowski, "Influence of temperature on the tribochemical reactions of hexadecane," *Lubrication Science,* vol. 15, pp. 329-340, 2003.

[31] V. Šmeļova, A. Schwedt, L. Wang, W. Holweger and J. Mayer, "Microstructural changes in White Etching Cracks (WECs) and their relationship with those in Dark Etching Region (DER) and White Etching Bands (WEBs) due to Rolling Contact Fatigue (RCF)," *International Journal of Fatigue,* vol. 100, no. 1, pp. 148-158, 2017.

[32] B. Gould, A. Greco, K. Stadler and X. Xiao, "An Analysis of premature cracking associated with microstructural alterations in an ASIS 52100 failed wind turbine bearing using X-ray tomography," *Materials and Design,* no. 117, pp. 417-429, 2017.

[33] T. Haque, S. Korres, J. T. Carey, P. W. Jacobs, J. Loos and J. Franke, "Lubricant effects on white etching cracking failures in thrust bearing rig tests," *Tribology Transactions,* vol. 61, no. 6, pp. 979-990, 2018.

[34] B. Gould, N. Demas, G. Pollard, J. J. Rydel, M. Ingram and A. C. Greco, "The effect of lubricant composition on white etching crack failures," *Tribology Letters,* vol. 67, no. 1, 2018.

[35] N. Kino and K. Otani, "The influence of hydrogen on rolling contact fatigue life and its improvement," *JSAE Review,* vol. 24, pp. 289-294, 2003.

[36] A. Maduako, G. Ofunner and C. Ojinnaka, "The role of metals in the oxidative degradation of automotive crankcase oils," *Tribology International,* vol. 29, no. 2, pp. 153-160, 1996.